

Effect of the $H_2O/Al_2(SO_4)_3$ ratio on physical properties in the synthesis of porous $AlO(OH)$ nano gel by homogeneous precipitation

Byung Ki Park* and Jeong Min Jin

Energy Materials Research Center, Korea Research Institute of Chemical Technology, Daejeon 305-343, Korea

An $AlO(OH)$ nano gel has been used as a precursor of a ceramic material, a coating material and a catalyst. For these uses, not only control of the physiochemical properties for the particle morphology, pore characteristics and peptization but also studies of a synthetic method for the preparation of advanced application products were required. In this study, an $AlO(OH)$ nano gel was prepared through the aging and drying process of aluminum hydroxides gel precipitated by the neutralization of a dilute $NaOH$ solution and an $Al_2(SO_4)_3$ solution. In this process, optimum synthetic conditions of an $AlO(OH)$ nano gel having excellent pore volume from the effect of a $H_2O/Al_2(SO_4)_3$ mole ratio on gel precipitates has been studied. The $H_2O/Al_2(SO_4)_3$ mole ratio brought about numerous changes in crystal morphology, specific surface area, pore volume and pore size. The physiochemical properties for the $AlO(OH)$ nano gel were investigated using the XRD, TEM, TG/DTA, FT-IR and the N_2 BET method.

Key words: Porous material, Boehmite, γ -alumina, Catalyst, Alumina ceramic.

Introduction

Aluminum hydroxide, depending on the amount of structural water inside the crystal, can be divided into trihydrates such as gibbsite and bayerite, monohydrates such as boehmite and diasporite, and then anhydrides containing less than 1 mole of water molecule per 1 mole of Al_2O_3 . Among these, $AlO(OH)$, a monohydrate form, is a precursor of γ - Al_2O_3 and is used as a catalyst and adsorbent, and is also used as a precursor of structural ceramics and functional ceramic products [1-8]. In addition, it has been used as an adsorbent, carrier, and binder for ceramic forming. According to Farkas and Gado [9-10], the crystal structure of $AlO(OH)$ forms a unit lattice with oxygen atoms coordinated on the edge of an octahedron with an aluminum ion in the center, and the hydrogen bond is formed between these layers. $AlO(OH)$ contains 1.0~1.8 moles of water molecules per 1 mole of Al_2O_3 between the layers of chain-like $[AlO(OH)]_2$. The crystal size is about 5~10 nm and its X-ray diffraction pattern has a wide full width at half maximum with a very broad characteristic peak. $AlO(OH)$ has very high pre- dehydration BET surface area as much as $500\text{ m}^2/\text{g}$ and post-dehydration pore volume as much as 1.2 cc/g , and if calcinated at $400\sim 600^\circ\text{C}$, it shows a maximum 30wt% weight reduction due to the break away of structural water and surface-adsorbed water and then a phase transition to γ - Al_2O_3

is observed. Boehmite with such characteristics can be manufactured by the hydrothermal reaction of gibbsite or bayerite, but is generally manufactured by the following three methods such as fast calcination in which amorphous alumina obtained through rapid pyrolysis of gibbsite is hydrated, neutralization in which aluminum salt solution is hydrolyzed as in this study, and the alkoxide method in which aluminum organic metal is hydrolyzed. The physical properties such as crystal morphology, BET surface area, pore volume, and pore size should be well controlled to increase the catalytic activity and adsorption characteristics of porous $AlO(OH)$, and when manufacturing porous $AlO(OH)$ by homogeneous precipitation, the physical properties are greatly changed depending on the mole ratio of $H_2O/Al_2(SO_4)_3$, precipitation pH, aging temperature, and aging time. An $Al_2(SO_4)_3$ solution has been mainly used as the flocculant for water treatment and is present in two concentrations, 23.5% and 27.8%, as $Al_2(SO_4)_3$ anhydride, and can be easily purchased. This $Al_2(SO_4)_3$ solution has been currently used only as the flocculant without any other usage and thus it is necessary to develop higher value-added ceramic and chemical products using this material. In this study, the effect of the $H_2O/Al_2(SO_4)_3$ mole ratio on the properties of porous $AlO(OH)$ nano gel was investigated using XRD, TG/DTA, FTIR, TEM, and N_2 BET methods when the $AlO(OH)$ nano gel was synthesized through aging after the $Al_2(SO_4)_3$ solution was neutralized by sodium hydroxide solution to gel precipitation.

*Corresponding author:
Tel : +82-42-860-7022
Fax: +82-42-861-4245
E-mail: bkpark@kriict.re.kr

Experiment Methods

Starting material & experiment equipments

Raw materials for the synthesis of porous $AlO(OH)$ nano gel were $Al_2(SO_4)_3$ solution (23.5%, flocculant for water treatment) and an alkaline source for neutralization, a 3M solution of sodium hydroxide (NaOH, Jin Chem., 99%) diluted in distilled water. Reaction equipments used were a 2l 3-neck flask with heating mantle (MS-DM604) attached and a microprocessor peristaltic pump (model 7014-10) for homogeneous precipitation of porous $AlO(OH)$ nano gel.

Experiment methods

To investigate the $H_2O/Al_2(SO_4)_3$ mole ratio for optimal pore characteristics, each aluminum sulfate solution with $H_2O/Al_2(SO_4)_3$ mole ratios of 190, 285, 380, or 475 was made while adding and stirring distilled water with a speed of 25 cc/minute to a 23.5% aluminum sulfate solution and then 3M NaOH solution was dropped with a speed of 25 cc/minute until the pH became 10.5 using a microprocessor peristaltic pump at room temperature. Then the temperature of the precipitates was increased to 90°C and the precipitates were aged for 24 hours, filtered and washed, and then dried at 110°C for 24 hours to obtain the $AlO(OH)$ nano gel. At this time, if the $H_2O/Al_2(SO_4)_3$ mole ratio was over 475, then it was difficult to obtain gel precipitation because the concentration of aluminum sulfate was too low, and if the water/aluminum sulfate mole ratio was less than 190, the viscosity of the precipitating gel rapidly increased to inhibit the continuous precipitation of $AlO(OH)$ nano gel. The experimental procedure is shown in Fig. 1.

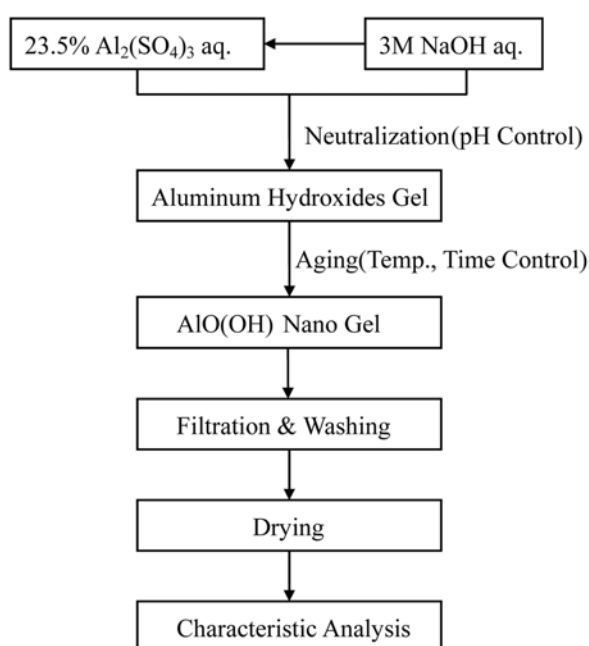


Fig. 1. Flow diagram for preparation of porous $AlO(OH)$ nano gel.

Analysis instruments

The gel was analyzed using a X-ray diffractometer (XRD, Rigaku Denki) with an interval of 0.02° and a scan speed of $5^\circ/\text{minute}$, in the range of $5^\circ \leq 2\theta \leq 80^\circ$, to identify the crystal structure of the gel precipitates. The absorption spectrum was analyzed in the frequency range of $400\sim 4,000\text{ cm}^{-1}$ using a Fourier Transform Infrared Spectrometer (FT-IR, MIDAC GRAMS 386) to examine O-H, Al-O, Al-OH, and H-O-H bonding structures of the gel precipitates. Differential thermal analysis was performed by heating up to $1,200^\circ\text{C}$ with a heating rate of 5K minute^{-1} in an air atmosphere to examine the ignition loss and phase transition temperature of the gel precipitates. Morphological changes of crystal grains were observed by a transmission electron microscope (TEM, TECNAI G²) and changes of BET surface area, pore volume, and pore size were measured by the N_2 BET method (ASAP 2000, Micro. Inst.).

Results & Discussion

Morphological changes in crystal structure & grains

X-ray diffraction angles of $AlO(OH)$ containing 1.0~1.8 moles of water molecules per 1 mole of Al_2O_3 were 14.4° , 28.2° , 38.3° , 48.9° , 64.1° , and 72.0° from the (020), (120), (140), (031), (200), and (051) crystal planes, respectively, and only the intensity of diffraction maxima was changed depending on the amount of structural water. Fig. 2 shows the results of XRD analysis of samples by changes of the $H_2O/Al_2(SO_4)_3$ mole ratio. In the case of (a) and (b), the crystals were not well developed and $AlO(OH)$ crystals with very low X-ray diffraction maxima were formed, whilst in (c), $AlO(OH)$ precipitates with well-developed crystals were formed, and in (d), mostly bayerite crystals were precipitated. In the TEM micrographs shown in Fig. 3, as in the case of (a), the needle-like crystals were small and thin when the $H_2O/Al_2(SO_4)_3$ mole ratio was low but increased in their length and width as the $H_2O/Al_2(SO_4)_3$ mole ratio increased. As shown in Table 1, this was because, as the amount of water increased, the final pH of the solution increased and the activation

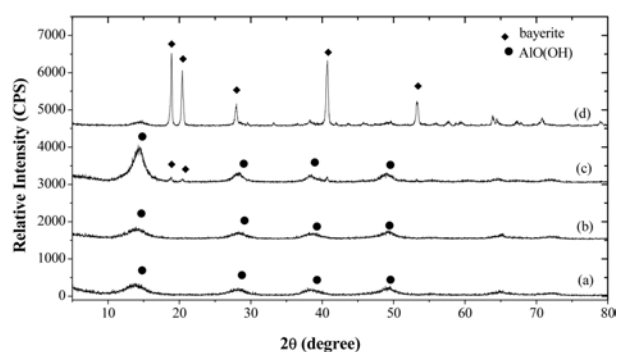


Fig. 2. XRD patterns of gel precipitates as a function of the $H_2O/Al_2(SO_4)_3$ mole ratio: (a) 190, (b) 285, (c) 380 and (d) 475.

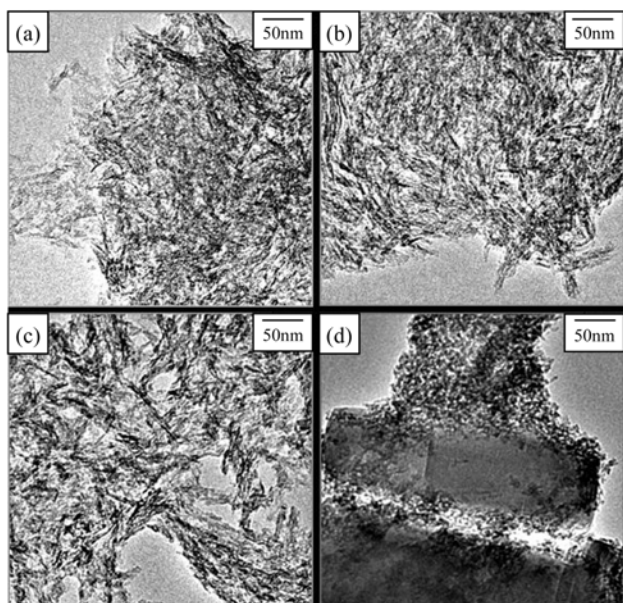


Fig. 3. TEM micrographs of gel precipitates as a function of the $\text{H}_2\text{O}/\text{Al}_2(\text{SO}_4)_3$ mole ratio: (a) 190, (b) 285, (c) 380 and (d) 475.

Table 1. Change of Final pH of $\text{AlO}(\text{OH})$ Nano Gel Prepared at Various $\text{H}_2\text{O}/\text{Al}_2(\text{SO}_4)_3$ Mole Ratios.

$\text{H}_2\text{O}/\text{Al}_2(\text{SO}_4)_3$ Mole Ratio	Aging Time (at 90°C)	Initial pH	Final pH
190	24h	10.5	8.13
285	24h	10.5	8.41
380	24h	10.5	9.84
475	24h	10.5	11.83

energy for crystal growth increased, and thus small and thin needle-like crystals were rapidly grown, and condensation among grains was developed as time passed [11, 13-18]. Also, the crystal growth of gel particles formed in the aqueous solution is determined by the OH^- existing between layers of $[\text{AlO}(\text{OH})]_2$, and the lower the initial pH and final pH of hydrolysis and the lower the $\text{H}_2\text{O}/\text{Al}_2(\text{SO}_4)_3$ mole ratio, more OH^- ions existed between the layers of $[\text{AlO}(\text{OH})]_2$ and the distance between the layers is increased to induce the distortion of $[\text{AlO}(\text{OH})]_2$ layers and to slow down the crystal growth [12]. It is thought that the density of the precipitated gel is increased as the $\text{H}_2\text{O}/\text{Al}_2(\text{SO}_4)_3$ mole ratio is lowered and the OH^- existing in the $[\text{AlO}(\text{OH})]_2$ layers are condensed to decrease the separation distance and thus to inhibit the crystal growth. However, when the $\text{H}_2\text{O}/\text{Al}_2(\text{SO}_4)_3$ mole ratio was increased and the final pH of hydrolysis was over 11, the precipitated gel was re-dissolved and re-crystallized into bayerite with the $\text{Al}(\text{OH})_3$ structure as shown in X-ray diffraction patterns in Fig. 2 and the TEM micrograph in Fig. 3(d). Changes in weight loss and temperature difference by the heating temperature are shown in Fig. 4 and Fig. 5. In these figures, gel precipitates obtained by neutralization and aging in the 190-380 range of the $\text{H}_2\text{O}/\text{Al}_2(\text{SO}_4)_3$ mole

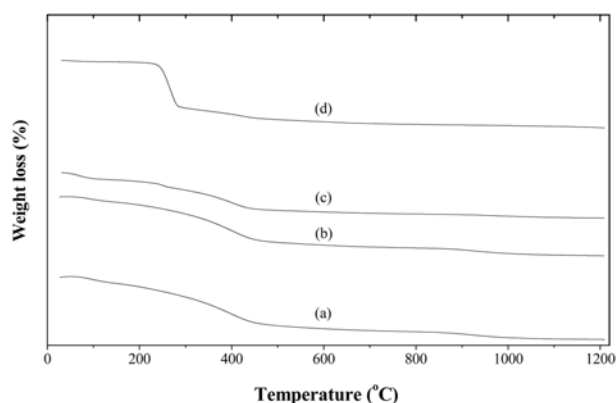


Fig. 4. TG curves of gel precipitates as a function of the $\text{H}_2\text{O}/\text{Al}_2(\text{SO}_4)_3$ mole ratio: (a) 190, (b) 285, (c) 380 and (d) 475.

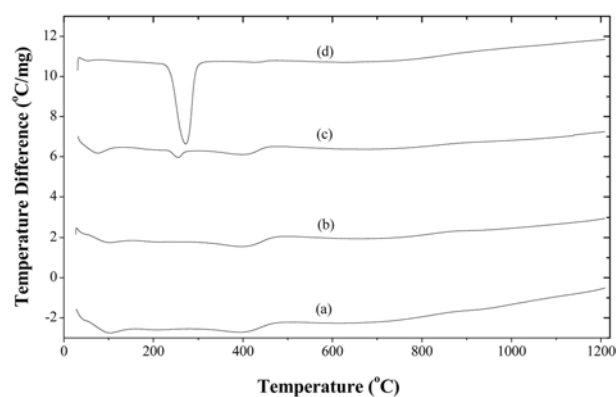


Fig. 5. DTA curves of gel precipitates as a function of the $\text{H}_2\text{O}/\text{Al}_2(\text{SO}_4)_3$ mole ratio: (a) 190, (b) 285, (c) 380 and (d) 475.

ratio had endothermic peaks near 400°C, which was a phase transition to $\gamma\text{-Al}_2\text{O}_3$ by condensing OH^- existing inside the $\text{AlO}(\text{OH})$ crystal and becoming separated as water. When the $\text{H}_2\text{O}/\text{Al}_2(\text{SO}_4)_3$ mole ratio was 380, there were small endothermic peaks near 260°C and 400°C at the same time. The peak near 260°C was due to the phase transition of bayerite into $\eta\text{-Al}_2\text{O}_3$ and the peak near 400°C was due to the phase transition of $\text{AlO}(\text{OH})$ into $\gamma\text{-Al}_2\text{O}_3$. Thus when the $\text{H}_2\text{O}/\text{Al}_2(\text{SO}_4)_3$ mole ratio was 380, not only were $\text{AlO}(\text{OH})$ crystals precipitated mostly but also a small amount of bayerite was precipitated at the same time. Therefore, gradual recrystallization into bayerite is thought to occur from the point when the $\text{H}_2\text{O}/\text{Al}_2(\text{SO}_4)_3$ mole ratio was 380 and over.

Changes in infrared absorption spectrum

The crystal structure of the gel precipitates as a function of the $\text{H}_2\text{O}/\text{Al}_2(\text{SO}_4)_3$ mole ratio was identified by Fourier Transform Infrared Spectroscopy in addition to XRD analysis. Fig. 6 showed the results of FT-IR spectra of gel precipitate samples produced and dried at 110°C for 24 hours. The absorption bands of $\text{AlO}(\text{OH})$ were largely divided into the one formed by adsorbed water at 3,800-2,400 cm^{-1} , the O-H stretching vibration

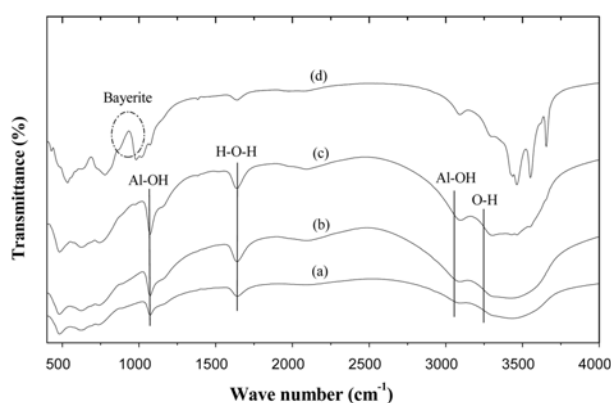


Fig. 6. FT-IR spectra of gel precipitates as a function of the $H_2O/Al_2(SO_4)_3$ mole ratio: (a) 190, (b) 285, (c) 380 and (d) 475.

peak by water present in the pore or water of hydration near $1,630\text{ cm}^{-1}$, the O-H bending vibration peak at $1,300\text{--}1,000\text{ cm}^{-1}$, and the Al-O vibration peak at $1,000\text{--}400\text{ cm}^{-1}$ [15–18]. The absorption band at $3,290\text{ cm}^{-1}$ with the $H_2O/Al_2(SO_4)_3$ mole ratio of 190–380 was made by adsorbed water (O-H), and the absorption bands at $3,100\text{ cm}^{-1}$ and $1,071\text{ cm}^{-1}$ were made by the Al-OH bending vibration within the $AlO(OH)$ crystal [12]. The absorption band near $1,635\text{ cm}^{-1}$ appeared from free water with the H-O-H structure, which was water present in the pores or water of hydration, and the absorption band at $2,090\text{ cm}^{-1}$ appeared due to the weak O-H hydrogen bond [15]. Then 3 absorption bands appeared in the frequency band less than 800 cm^{-1} were ones appearing in both $AlO(OH)$ and bayerite [12]. The absorption bands at 879 cm^{-1} and 979 cm^{-1} appeared when the $H_2O/Al_2(SO_4)_3$ mole ratio was 475, were made by the formation of bayerite [12]. As a result, it was confirmed that when the $H_2O/Al_2(SO_4)_3$ mole ratio was in the range of 190–380, $AlO(OH)$ was formed, but when it was over 475, bayerite was formed. This was consistent with the XRD analysis results in Fig. 2 and with the TEM analysis results in Fig. 3.

Changes in specific surface area & pore structure

Fig. 7 showed the plots of BET surface areas of gel precipitates as a function of the $H_2O/Al_2(SO_4)_3$ mole ratio using N_2 ads./des. isotherm at liquid nitrogen temperature. When the $H_2O/Al_2(SO_4)_3$ mole ratio was less than 380, the shape of the isotherms showed that the adsorption volume was low and hysteresis was developed in which the adsorption/desorption curve was not consistent at a low relative pressure. This phenomenon was observed when the $H_2O/Al_2(SO_4)_3$ mole ratio was low because the density of the gel was increased and the final pH of gel precipitates was decreased and the activation energy for $AlO(OH)$ crystal growth was lowered resulting in crystals that were not developed and many micro-pores existed. Therefore, as shown in Table 2, the BET surface area from micro-pores increased but the overall pore

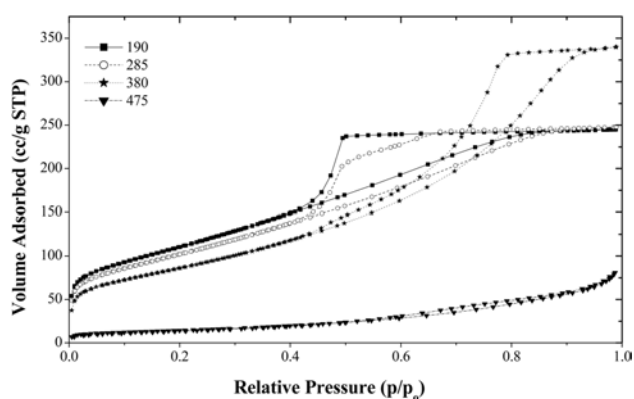


Fig. 7. N_2 ads./des. isotherm of gel precipitates as a function of the $H_2O/Al_2(SO_4)_3$ mole ratio.

Table 2. Physical Properties of $AlO(OH)$ Nano Gel Prepared at Various $H_2O/Al_2(SO_4)_3$ Mole Ratios.

$H_2O/Al_2(SO_4)_3$ Mole Ratio	BET Surface Area (m^2/g)	Pore Volume (cc/g)	Pore Diameter (\AA)
190	400.88	0.37	37.81
285	370.56	0.38	41.40
380	312.37	0.53	67.35
475	51.45	0.13	97.22

volume tended to decrease. While in the case when the $H_2O/Al_2(SO_4)_3$ mole ratio was as high as 475, the density of gel decreased and the final pH of the gel increased over 11 and the gel was re-dissolved in the aqueous solution to be precipitated as compact bayerite crystals with almost no pores. As shown in the pore size distributions in Fig. 8 and the X-ray diffraction patterns in Fig. 2, when the $H_2O/Al_2(SO_4)_3$ mole ratio was less than 380, the crystal growth of $AlO(OH)$ was slowed down and pores were mainly in the range of 30–40 \AA , but when $AlO(OH)$ crystals were well developed as in the case when the $H_2O/Al_2(SO_4)_3$ mole ratio was 380, pores in the range of 30–40 \AA grew to be pores in the range of 50–100 \AA . But almost no pores existed when the $H_2O/Al_2(SO_4)_3$ mole ratio was 475.

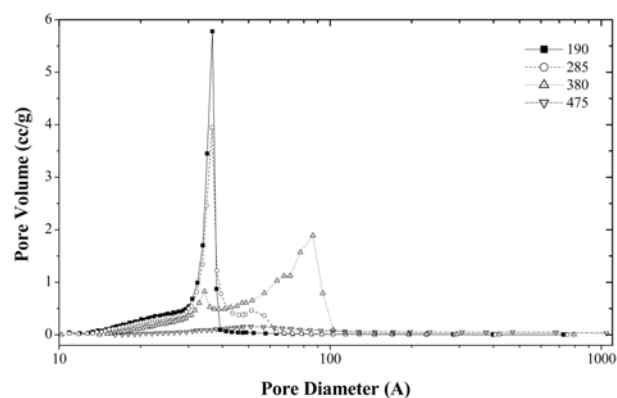


Fig. 8. Pore size distributions of gel precipitates as a function of the $H_2O/Al_2(SO_4)_3$ mole ratio.

Conclusions

When porous AlO(OH) nano gel was synthesized through aging after an Al₂(SO₄)₃ solution was neutralized by sodium hydroxide solution, gel precipitates were affected by the H₂O/Al₂(SO₄)₃ mole ratio, and the following conclusions were obtained.

1. When the H₂O/Al₂(SO₄)₃ mole ratio was in the range of 190~380, porous boehmite with a chemical composition of AlO(OH) was precipitated, and when the H₂O/Al₂(SO₄)₃ mole ratio was over 475, almost non-porous bayerite with the Al(OH)₃ structure was formed.

2. As the H₂O/Al₂(SO₄)₃ mole ratio was increased to 190~380, the BET surface area was decreased from 401 m²/g to 312 m²/g and the average pore size was increased from 37 Å to 67 Å and the pore volume was also increased from 0.37 cc/g to 0.53 cc/g.

3. When the H₂O/Al₂(SO₄)₃ mole ratio was 380 and the gel precipitates were aged at 90°C for 24 hours, a porous AlO(OH) nano gel with a maximum pore volume of 0.53 cc/g could be formed.

References

1. R. K. Oberlander, *Appl. Ind. Catalysis*, 3 (1984) 63-110.
2. P. Nortier and M. Soustelle, ed. by Crucq and A. Frennet, Elsevier Sci. Pub. (1987) 275-300.
3. R. B. Bagwell and G. L. Messing, *Key Eng. Mater.*, 115 (1996) 45-64.
4. C. Misra, *Encyclopedia of Chem. Tech.*, 4th ed., 2 (1992) 317-330.
5. L. K. Hudson, C. Misra and K. Wefers, *Ullmann's Encyclopedia of Ind. Chem.*, 5th ed., (1985) 557-594.
6. B. C. Lippens and J. J. Steggerda, *Physical and Chemical Aspects of Adsorbents and Catalysts*, 4 (1970) 171-211.
7. R. Dale Woosley, *Alumina Chemicals*, 2nd ed., Am. Ceram. Soc., (1990) 241-250.
8. W. A. Deer, R. A. Howie, and J. Zussman, *Longmans*, London, 5 (1969) 111-116.
9. L. Farkas, P. Gado, and P.E. Wermer, *Mat Res. Bull.*, 12 (1977) 1213-1218.
10. B. K. Park, J. K. Suh, J. M. Lee and D. S. Suhr, *J. Kor. Ceram. Soc.*, 35 [10] (1998) 1085-1093.
11. S. Ram, *Infrared Physics & Technology* 42 (2001) 547-560.
12. K. H. Lee, B. H. Ha, *J. Korea Institute Chem. Eng.*, 34(1), (1996) 28-35.
13. U. S Patent: 4,391,740 (1983).
14. B. K. Park, J. K. Suh, J. M. Lee and D. S. Suhr, *J. Kor. Ceram. Soc.*, 39 [3] (2002) 245-251.
15. Z. J. Galas, S. Janiak, W. Mista, J. Wrzyszczy and M. Zawadzki, *J. Mat. Sci.*, 28 (1993) 2075-2078.
16. B. K. Park, J. M. Lee, and D. S. Suhr, *J. Kor. Ceram. Soc.*, 40 [7] (2003) 683-89.
17. B. K. Park, J. M. Lee, and D. S. Suhr *J. Kor. Ceram. Soc.*, 40 [8] (2003) 758-64.
18. B. K. Park, J. K. Suh, and J. M. Lee, *J. Kor. Ceram. Soc.*, 42 [4] (2005) 237-44.